

# RSC Advances



This is an *Accepted Manuscript*, which has been through the Royal Society of Chemistry peer review process and has been accepted for publication.

*Accepted Manuscripts* are published online shortly after acceptance, before technical editing, formatting and proof reading. Using this free service, authors can make their results available to the community, in citable form, before we publish the edited article. This *Accepted Manuscript* will be replaced by the edited, formatted and paginated article as soon as this is available.

You can find more information about *Accepted Manuscripts* in the [Information for Authors](#).

Please note that technical editing may introduce minor changes to the text and/or graphics, which may alter content. The journal's standard [Terms & Conditions](#) and the [Ethical guidelines](#) still apply. In no event shall the Royal Society of Chemistry be held responsible for any errors or omissions in this *Accepted Manuscript* or any consequences arising from the use of any information it contains.

## ARTICLE

Dynamic motion of Lu pair inside  $C_{76}(T_d)$  cage

v Juanyuan Hao,<sup>a</sup> Fengyu Li,<sup>b</sup> Hongjiang Li,<sup>a</sup> Xiaoyu Chen,<sup>a</sup> Yuyan Zhang,<sup>a</sup> Zhongfang Chen,<sup>b</sup> Ce Hao<sup>\*a</sup>

Cite this: DOI: 10.1039/x0xx00000x

Received 00th January 2014,  
Accepted 00th January 2014

DOI: 10.1039/x0xx00000x

www.rsc.org/

The relativistic density functional theory (DFT) computations were performed to investigate the dynamic motion of encapsulated Lu pair inside  $C_{76}(T_d)$  cage. The results revealed that the lowest-energy configuration of  $Lu_2@C_{76}(T_d)$  adopts  $C_2$  symmetry, four electrons are transferred to the outer carbon cage and the two encapsulated Lu atoms form a metal-metal single bond (with an electronic structure of  $Lu_2^{4+}@C_{76}^{4-}$ ), and the good electron delocalization in the  $C_{76}^{4-}(T_d)$  cage partially contributes the thermodynamic preference of  $Lu_2@C_{76}(T_d)$ . The rather small barrier (3.2 kcal/mol) for  $Lu_2$  atoms to hop from one stable site to another leads to flexible motion of Lu pair inside the parent fullerene cage, and the  $O_h$  symmetrical motion trajectory of two Lu atoms is consistent with the STM image. The computed  $^{13}C$  NMR spectrum with this trajectory also well agrees with the experimental results.

## Introduction

Endohedral metallofullerenes (EMFs) have rather unique properties unexpected in empty fullerenes.<sup>1-3</sup> These properties lead to the wide applications of EMFs in various fields, such as materials science, energy, medicine, etc.<sup>4-11</sup> Especially, the dynamic behavior of encapsulated atoms in the cage endows EMFs as potential candidates for molecular and nano-devices.<sup>12</sup> Not surprisingly, many experimental and theoretical studies have been carried out to investigate the dynamic motion of encapsulated atoms in EMFs.<sup>13</sup> The scenario of La or Y atom moving inside  $C_{82}$  (with  $C_2$  symmetry) was firstly predicted by Andreoni and Curioni using *ab initio* molecular dynamics (MD) simulations.<sup>14</sup> Nishibori *et al.* provided the first experimental evidence of the La atom movement inside  $C_{82}$  cage, their maximum entropy method (MEM)/Rietveld analysis using synchrotron powder diffraction data indicated that La atom has a giant bowl-shaped movement at room temperature.<sup>15</sup> However, the DFT studies by Jin *et al.* revealed a conflicting picture,<sup>16</sup> they suggested that La atom undergoes a boat-shaped motion with a small amplitude inside  $C_{82}(C_{2v})$  fullerene cage, rather than the bowl or hemisphere model with a large amplitude obtained from MEM/Rietveld analysis.

$M_2@C_{80}$  ( $M=La,Ce$ ) are the representatives of dimetallofullerenes. For  $La_2@C_{80}(I_h)$ , two La atoms circulate three-dimensionally inside the  $C_{80}(I_h)$  cage, which was supported by the two carbon signals in  $^{13}C$  NMR spectrum and one peak in  $^{139}La$  NMR spectrum in experiments.<sup>17</sup> A deeper insight into the La pair motion was given by MEM/Rietveld analysis, which demonstrated that the two La atoms present a trajectory that connects the six-membered rings of  $C_{80}(I_h)$ , or a pentagonal-dodecahedron,<sup>18</sup> as well as by DFT computations.<sup>19</sup> For  $Ce_2@C_{80}(I_h)$ , its  $^{13}C$  NMR spectrum indicated that the Ce atoms circulate randomly, as La atoms do in  $La_2@C_{80}(I_h)$ .<sup>20</sup> The other isomer of  $Ce_2@C_{80}$ , which has a  $D_{5h}$   $C_{80}$  outer cage, was synthesized by Yamada *et al.*,<sup>21</sup> the  $^{13}C$  NMR analysis and DFT

computations revealed that the Ce atoms circulate two-dimensionally along a band of 10 contiguous hexagons inside the  $C_{80}(D_{5h})$  cage.

$C_{76}$  fullerene has two structural isomers ( $D_2$  and  $T_d$ ) satisfying the isolated pentagon rule (IPR). The pristine  $C_{76}(T_d)$  isomer has not been synthesized yet due to its inherent open shell electronic structure. Excitingly, in 2010, Umemoto *et al.* synthesized and isolated  $Lu_2@C_{76}$  for the first time.<sup>22</sup> The UV-Vis-NIR, STM and  $^{13}C$  NMR chemical shift analysis disclosed that the entire  $Lu_2@C_{76}$  molecule has  $T_d$  symmetry, and the charge state of  $(Lu_2)^{6+}@C_{76}^{6-}(T_d)$  was suggested. They also speculated that the two encapsulated Lu atoms rapidly rotate along a rhombic dodecahedron inside the cage to maintain the high symmetry. However, in 2011, by means of systematic density functional theory (DFT) computations and statistical thermodynamic analysis, Yang *et al.*<sup>23</sup> revealed that the inner two Lu atoms form a metal-metal single bond, and only transfer four electrons to the fullerene sphere, resulting in a formal valence state of  $(Lu_2)^{4+}@C_{76}^{4-}(T_d)$ ; they also suggested that the  $Lu_2$  dimer can hop rapidly between six equivalent configurations in the fullerene cage at room temperature, giving rise to a trajectory as a tetrahedron in  $C_{76}(T_d)$ . Such a controversy caught our interest: What is the most stable configuration for  $Lu_2@C_{76}$ ? What is its bonding nature? What is the energy barrier for the dynamic motion of Lu atoms? Is the motion scenario a rhombic dodecahedron or a tetrahedron<sup>22?</sup>

In this paper, by means of relativistic DFT computations, we first investigated different isomers of  $Lu_2@C_{76}$  and located the transition states for the Lu motion between the lowest-energy isomers. The bonding nature of the thermodynamically most favorable  $Lu_2@C_{76}(T_d)$  isomer was analyzed by quantum theory of atoms in molecules (QTAIM) method. Our computations support Yang *et al.*'s recent electronic structure assignment ( $Lu_2^{4+}@C_{76}^{4-}$ ). Then, by analyzing the partial trajectory of Lu atoms surrounding the molecular geometric center, we obtained the  $O_h$  symmetrical motion trajectory of two Lu atoms inside

$C_{76}$  cage. Furthermore, following the Lu motion trajectory, we calculated the  $^{13}\text{C}$  NMR spectrum of  $\text{Lu}_2@C_{76}$ . Both the computed Lu motion trajectory and  $^{13}\text{C}$  NMR spectrum agree well with the experimental measurement.

## Computational Methods

ADF2008.01 program<sup>24-26</sup> and DMol<sup>3</sup> code<sup>27</sup> were employed for the relativistic DFT calculations. The relativistic effects were taken into account by using the zero-order regular approximation (ZORA)<sup>28-30</sup> basis sets in ADF2008.01, as well as all electron relativistic core treatment in DMol<sup>3</sup>.

By ADF2008.01 program, full geometry optimizations without symmetry constraints were carried out using the generalized gradient approximation (GGA)<sup>31</sup> exchange-correlation functional BLYP<sup>32,33</sup> with a triple-zeta polarized (TZP) basis set (referred to as GGA-BLYP/TZP). In addition, the frozen-core approximation up to the 1s orbital for C atoms and the 5p orbital for Lu atoms was used. By DMol<sup>3</sup> code, geometry optimizations and transition state calculations were done at the GGA-BLYP/DNP level.

To disclose the bonding nature of  $\text{Lu}_2@C_{76}$ , we performed QTAIM analysis<sup>34,35</sup> of the most stable  $\text{Lu}_2@C_{76}$ . The wavefunction was generated at BLYP/6-31G\*~SDD<sup>36</sup> in Gaussian using the optimized geometries (BLYP/TZP in ADF). We also tested BLYP/6-31G\*~SARC<sup>37</sup> and BP86/6-31G\*~SARC<sup>32,33,38</sup> methods, and they gave very close results to that of BLYP/6-31G\*~SDD.

To better understand the inferred extraordinary electronic structure of  $\text{Lu}_2^{4+}@C_{76}^{4-}$ , we evaluated the electron delocalization (aromaticity) of the low-lying  $C_{76}^{4-}$  and  $C_{76}^{6-}$  isomers. Nucleus-independent chemical shifts (NICS,<sup>39,40</sup> in ppm), a simple and efficient method to evaluate aromaticity,<sup>39,40</sup> were computed at the cage centers of the optimized geometries of the empty cages with Gaussian 09 program.<sup>41</sup>

The  $^{13}\text{C}$  NMR spectrum was calculated using gauge-independent atomic orbital (GIAO) method<sup>42</sup> at the GGA-BLYP/TZP theoretical level by using the ADF2008.01 program. The chemical shifts were first evaluated relative to  $\text{C}_{60}$ , then were referenced to the carbon disulfide ( $\text{CS}_2$ ) ( $\delta(\text{C}_{60})$  143.15 ppm vs.  $\text{CS}_2$ ).<sup>43</sup>

## Results and Discussions

### Searching for the lowest-energy isomer and its bonding nature:

To clearly describe the symmetry of a  $C_{76}(T_d)$  cage, we take a triangle patch under a circum-spherical surface as a representative patch of the  $C_{76}(T_d)$  cage (Figure 1). The area of this patch is equal to 1/24 of the total  $C_{76}$  surface. On this representative patch, 16 key points are located at five kinds of carbon atoms (points C1, C2, C3, C4, C5), at seven kinds of bond center (point b1, b2, b3, b4, b5, b6, b7), at one five-membered ring's center (point p), and at three six-membered rings' centers (point h1, h2, h3). Every key point has its own local symmetry. For example, point L is at the intersectional carbon atom of three six-membered rings with  $C_{3v}$  local symmetry; point N is at the center of the six-membered ring with  $C_{3v}$  local symmetry; point M is at the center of 6-6 bond with  $C_{2v}$  local symmetry. We define point O as the geometric center of the carbon cage. Then the boundary of the patch can be characterized by a threefold axis OL, a two-fold axis OM and a three-fold axis ON. Note that all the independent symmetrical elements belonging to the  $T_d$  point group can be found in the representative patch. The entire surface of the polyhedron can be encompassed by performing different

elemental symmetry operations on the patch. Therefore, we can consider the patch LMN (shaded) as the smallest structural unit rather than the whole cage.

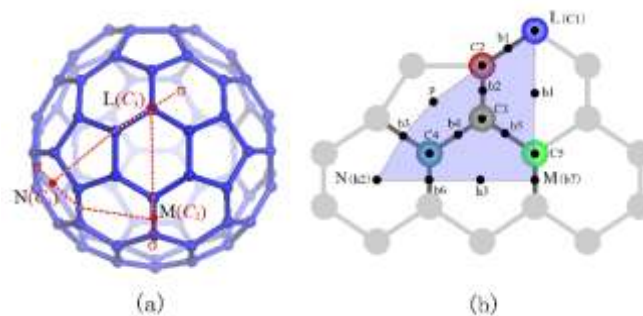


**Figure 1.** (a) the geometric structure of  $C_{76}(T_d)$  cage with the representative triangle LMN path; (b) all the key points on the patch: C1, b7 and h2 represent a three-fold axis, a two-fold axis, and a three-fold axis, respectively.

When the two Lu atoms are encapsulated in the cage, the system reduces from the original  $T_d$  symmetry of  $C_{76}$  to a lower symmetry depending on the relative positions of the two Lu atoms inside the cage. Corresponding to the key points in the representative patch, full geometry optimizations were carried out for all 16 possible isomers, which resulted in five configurations, referred to as  $C_2$ ,  $C_1$ ,  $C_s$ ,  $C_{3v}$  and  $D_{2d}$  according to the geometric symmetry. Table 1 summarizes the Lu-Lu distances ( $R_{\text{Lu-Lu}}$ ), the shortest Lu-C distances ( $R_{\text{Lu-C}}$ ), the relative energies and HOMO-LUMO gap energies for these five configurations of  $\text{Lu}_2@C_{76}$ . The results obtained by both ADF and DMol<sup>3</sup> are presented.

**Table 1.** Key geometric parameters, relative energies and HOMO-LUMO gap energies for the five configurations of  $\text{Lu}_2@C_{76}$ . The results outside and inside the parentheses are from ADF and DMol<sup>3</sup>, respectively.

Isomer	$R_{\text{Lu-Lu}}(\text{\AA})$	$R_{\text{Lu-C}}(\text{\AA})$	RelativeEnergy(k cal/mol)	Gap(eV)
$C_2$	3.36 (3.38)	2.42 (2.40)	0.0 (0.0)	0.75 (0.80)
$C_1$	3.40 (3.46)	2.48 (2.43)	1.8 (0.4)	0.74 (0.79)
$C_s$	3.45 (3.50)	2.49 (2.45)	5.4 (3.2)	0.70 (0.75)
$C_{3v}$	3.47 (3.50)	2.46 (2.42)	8.1 (4.7)	0.63 (0.72)
$D_{2d}$	3.36 (4.00)	2.44 (2.41)	25.5 (24.8)	0.49 (0.60)

ADF and DMol<sup>3</sup> give the same order of relative energies and HOMO-LUMO gaps for the five isomers. The  $C_2$  configuration is of the lowest energy and largest HOMO-LUMO gap. The thermodynamic stability is followed by the  $C_1$  and  $C_s$  isomers. The more symmetrical isomers,  $C_{3v}$  and  $D_{2d}$ , have rather high relative energies and smaller HOMO-LUMO gaps.

Figure 2 presents the top and side view of the  $C_2$  configuration, the lowest energy isomer of  $\text{Lu}_2@C_{76}$ . Though the  $R_{\text{Lu-Lu}}$  and  $R_{\text{Lu-C}}$  of the five isomers are pretty close (see Table 1), the  $C_2$  configuration has the smallest  $R_{\text{Lu-Lu}}$  and  $R_{\text{Lu-C}}$  (3.36 and 2.42  $\text{\AA}$ , respectively, by ADF; the corresponding values are 3.38 and 2.40  $\text{\AA}$  by DMol<sup>3</sup>).

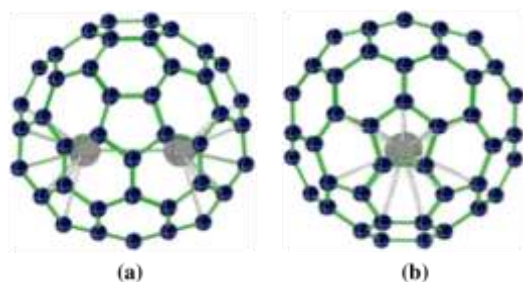


**Figure 2.** Top (a) and side (b) views of the lowest-energy isomer (with  $C_2$  symmetry) of  $\text{Lu}_2@C_{76}$ . Lu atoms are green balls and C atoms are gray.

In order to confirm the reliability of the predicted relative stabilities, especially the frozen-core approximation for the basis sets, we carried out additional optimizations for the  $C_2$  and  $C_{3v}$  isomers using three different function, namely GGA-BP86, PBE<sup>44</sup> and PW91<sup>45</sup>, together with the TZP all electron basis set using ADF package. The computational results summarized in Table 2 show that these function give rather similar optimized geometries and relative energies with those at GGA-BLYP/TZP. The  $R_{\text{Lu-Lu}}$  and  $R_{\text{Lu-C}}$  have almost no change, the biggest differences are within 0.03 Å. The relative energy difference between the two isomers is nearly the same, the  $C_2$  configuration is about 11 kcal/mol lower than that of the  $C_{3v}$  configuration. Therefore, we can expect that the employed BLYP functional and the TZP basis set with frozen-core approximation can result in reasonable structures and energies of all the configurations.

**Table 2.** Computed key geometric parameters and relative energies of the  $C_2$  and  $C_{3v}$  isomers with different function.

Method	Isomer	$R_{\text{Lu-Lu}}(\text{Å})$	$R_{\text{Lu-C}}(\text{Å})$	Relative Energy (kcal/mol)
BP	$C_2$	3.37	2.40	0.0
	$C_{3v}$	3.49	2.44	11.5
PBE	$C_2$	3.38	2.40	0.0
	$C_{3v}$	3.50	2.44	10.6
PW91	$C_2$	3.37	2.40	0.0
	$C_{3v}$	3.49	2.44	11.3

The key point of the controversy about the electronic structure assignment ( $(\text{Lu}_2)^{6+}@C_{76}^{6-}$  by Umemoto *et al.* vs.  $(\text{Lu}_2)^{4+}@C_{76}^{4-}$  by Yang *et al.*) is whether the two encapsulated Lu atoms form a single bond. To address this issue, we performed QTAIM analysis, which is a well-established method to analyze the topology of the electron density, and has been used for revealing and quantifying the bonding situation between the metal atoms and carbon cage in EMFs.<sup>46-53</sup> The result of the above obtained lowest-energy isomer of  $\text{Lu}_2@C_{76}$  was shown in Figure 3. Herein we focus on the encapsulated Lu atom pair. Our computations showed that there is one Lu-Lu bond critical point (BCP). The small values of electron density  $\rho_{\text{bcp}}$  (0.058 a.u.) and Laplacian  $\nabla^2\rho_{\text{bcp}}$  (0.005 a.u.) suggest weak covalent interaction between the two Lu atoms. The covalent nature is further confirmed by the negative total energy density ( $-0.021$  a.u.) and the small ratio of the kinetic energy density  $G$  to  $\rho$  ( $< 1$ ). The covalent bonding between the encapsulated Lu pairs leads to the formal valence state of  $\text{Lu}_2^{4+}@C_{76}^{4-}$ , instead of  $\text{Lu}_2^{6+}@C_{76}^{6-}$ .

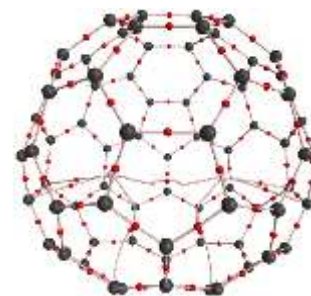


**Figure 3.** Molecular graphs of the most stable  $\text{Lu}_2@C_{76}$  (C and Lu atoms are black and white balls, respectively, the BCPs are the tiny spheres in red). Ring and cage CPs are omitted for clarity.

With the formal valence state of  $\text{Lu}_2^{4+}@C_{76}^{4-}$ , four electrons should be transferred from the encapsulated Lu pair to the outer  $C_{76}$  cage. What factor is stabilizing the  $C_{76}$  ( $T_d$ ) tetranion? Noting that aromaticity is playing an important role to stabilize spherical clusters,<sup>54,55</sup> we compared the relative energies and computed the NICS values at the structural centers of low-lying  $C_{76}^{4-}$  and  $C_{76}^{6-}$  isomers (Table 3). Our computed relative energies are in good agreement with those reported by Yang *et al.* Among the four structural isomers we considered, the hexanions of three isomers (with  $D_2$ ,  $C_{2v}$  and  $C_s$  symmetry) have more negative NICS values, thus higher aromaticity, than the corresponding tetranions. The only exception is the  $T_d$  isomer, its  $C_{76}^{4-}$  has more negative NICS value than  $C_{76}^{6-}$ , implying the stronger aromaticity of  $C_{76}^{4-}$  ( $T_d$ ), which should be partially responsible for its higher stability (Table 3), and echoes gracefully the formal valence state of  $\text{Lu}_2^{4+}@C_{76}^{4-}$  instead of  $\text{Lu}_2^{6+}@C_{76}^{6-}$ .

The partial charges on the two Lu atoms obtained from our natural population analysis are both +1.5 |e|. The large charge transfer phenomena were also found in other EMFs.<sup>56,57</sup> For example, Popov and Dunsch's comprehensive theoretical analyses found that the metal atom charges in  $M_3N@C_{2n}$  ( $M = \text{Sc}, \text{Y}, \text{La}$ ) are in the range of +1.6 ~ +1.9 |e|, the electronic structure of  $(M_3N)^{6+}@C_{2n}^{6-}$  was assigned.<sup>57</sup>

**Table 3.** Computed relative energies (at B3LYP/6-31G\*) and NICS values (at GIAO-B3LYP/6-31G\*\*/B3LYP/6-31G\*) of  $C_{76}^{4-}$  and  $C_{76}^{6-}$  isomers.

$C_{76}$ spiral ID	PG	PA	$C_{76}^{4-}$		$C_{76}^{6-}$	
			$\Delta E$ (kcal/mol)	NICS (ppm)	$\Delta E$ (kcal/mol)	NICS (ppm)
19151	$T_d$	0	0.00	-7.93	6.83	-5.79
19150	$D_2$	0	37.87	-12.91	31.58	-18.21
19138	$C_{2v}$	1	17.12	-4.96	4.55	-14.00
17490	$C_s$	2	20.74	-11.36	0.00	-20.10

### The transition state and motion trajectory:

In Umemoto *et al.*'s study,<sup>22</sup> they speculated that Lu atoms in the  $C_{76}$  cage move rapidly in a rhombic dodecahedron trajectory to maintain the molecule's  $T_d$ -symmetry. However, Yang *et al.*<sup>23</sup> suggested that a tetrahedron trajectory. What is the true trajectory?

In order to compute the trajectory of Lu atoms, we located the molecular transition state between two optimized  $C_2$  configurations. The obtained transition state has a  $C_s$  symmetry, the two Lu atoms are separated by 3.75 Å, and the smallest distance between Lu and the carbon cage is 2.42 Å. Figure 4a and Figure 4b are the top and side views of the transition state structure, respectively. The nature of the transition state was characterized by the only imaginary frequency of 54.8i  $\text{cm}^{-1}$  in the DMol<sup>3</sup> computations. The activation barrier is only 3.2

kcal/mol, which indicates that the two Lu atoms can hop from one  $C_2$  point to another around the geometric center of carbon cage. On the basis of these data, we can get the partial trajectory that Lu atoms move inside the cage along the lowest energy path, as shown in Figure 4c. We can further achieve the full motion trajectory by performing all the symmetry operations of  $T_d$  group to the partial trajectory based on the representative patch of the  $C_{76}$  ( $T_d$ ). The obtained trajectory is a rhombic dodecahedron with  $O_h$  symmetry (Figure 4d). Note that eight apexes of the trajectory are small planes consisting of Lu atoms (pointing to h1 or C1 in the representative patch), and they look like truncated corners. The motion trajectory of two Lu atoms is consistent with the STM image in Umemoto *et al.*'s study.

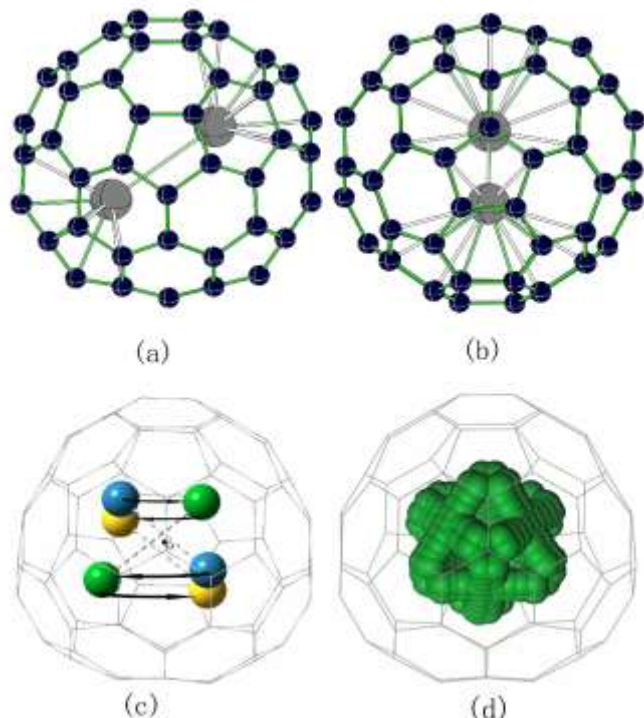


**Figure 4.** Top (a) and side (b) views of the transition state structure; (c) the lowest energy path for the Lu atoms to hop between lowest-energy configurations, the blue balls represent the started  $C_2$  isomer, the green balls represent  $C_s$  isomer in transition state, the yellow balls represent the terminated  $C_2$  isomer, the arrow represent the motion direction; (d) the complete motion trajectory of Lu atoms in  $C_{76}$  carbon cage.

Why does the motion trajectory have  $O_h$  symmetry when it is operated in the  $T_d$  group? There are two reasons:

1. Not considering the outer  $C_{76}$  ( $T_d$ ) carbon cage, the two Lu atoms are always moving around the center of symmetry  $i$ , which coincides with the geometric center  $O$ . By the symmetry operation:

$$S_4 \cdot i = C_4, \quad C_3 \cdot i = S_6$$

All the symmetry operations of  $T_d$  group associated with the center inversion will generate the  $O_h$  symmetry.

2. When taking the carbon cage into consideration, the  $Lu_2@C_{76}$  molecule will show  $T_d$  symmetry due to the fast motion of Lu atoms inside the fullerene cage. As the  $T_d$  group is a subgroup of  $O_h$  group, the motion trajectory of Lu atoms can be reduced from  $O_h$  to  $T_d$  in the molecule. This trajectory is in good agreement with the experimental STM images.<sup>22</sup>

### $^{13}C$ NMR spectrum:

Utilizing the representative patch of the  $C_{76}$  ( $T_d$ ), the  $^{13}C$  NMR spectra of  $C_{76}$  ( $T_d$ ) and  $Lu_2@C_{76}$  can be qualitatively discussed. There are five kinds of carbon atoms (points C1, C2, C3, C4, C5) in the patch, thus,  $^{13}C$  NMR spectrum should have five peaks. Points C3 and C4 should give full intensity signals because of their local  $C_1$  symmetry. In comparison, points C2 and C5 should present semi-intensity signals since they both have a mirror plane and local  $C_s$  symmetry, while with two mirror planes and a triple-axis, point C1 can only give 1/6 intensity signal due to its local  $C_{3v}$  symmetry. Based on the above analysis, the  $^{13}C$  NMR spectra of  $C_{76}$  ( $T_d$ ) and  $Lu_2@C_{76}$  should have five peaks: two full intensity signals, two semi-intensity signals and one 1/6 intensity signal.

To simulate the dynamic  $^{13}C$  NMR spectrum of  $Lu_2@C_{76}$  quantitatively, we computed the average chemical shifts for all of the carbon atoms and identified their status. According to the representative patch of the  $C_{76}$  ( $T_d$ ), carbon atoms are classified and their arithmetic average chemical shifts are calculated. The computed  $^{13}C$  chemical shifts and intensities are 126.55 ppm (C1 intensity 1), 134.36 ppm (C3, intensity 6), 135.51 ppm (C2, intensity 3), 140.72 ppm (C5, intensity 3), and 141.01 ppm (C4, intensity 6), which agree very well with the experimental data (Table 4) and those predicted by Yang *et al.*<sup>23</sup>

**Table 4.** Comparison between the calculated and experimentally measured  $^{13}C$  NMR of  $Lu_2@C_{76}$  ( $T_d$ ) chemical shifts ( $\delta_{cal}$  and  $\delta_{exp}$ ) and intensities ( $I_{cal}$  and  $I_{exp}$ ). The experimental results are from Ref. 22.

No.	$\delta_{cal}$	$\delta_{exp}$	$I_{cal}$	$I_{exp}$	C
1	126.55	129.61	1	1.00	C1
2	134.36	134.51	6	6.67	C3
3	135.51	137.85	3	3.18	C2
4	140.72	140.65	3	3.23	C5
5	141.01	142.39	6	6.55	C4

All the experimental data showed that  $Lu_2@C_{76}(T_d)$  has  $T_d$  symmetry,<sup>22</sup> while our computations and those by Yang *et al.*<sup>23</sup> showed that its lowest-energy isomer has  $C_2$  symmetry. How can we reconcile this discrepancy?

First we need to keep in mind that the experimentally measured UV-Vis-NIR, STM and  $^{13}C$  NMR chemical shifts present only the average result of the motion of Lu atoms in  $C_{76}$  cage. Actually, two stable sites for Lu atoms exist inside  $C_{76}(T_d)$  cage, which leads to the lowest-energy isomer with  $C_2$  symmetry. The small activation barrier (3.2 kcal/mol) enables these two Lu atoms hop between the two energetically most preferred sites inside  $C_{76}(T_d)$ . Thus, it is the dynamical motion behavior of Lu atoms along the rhombic dodecahedron trajectory (with  $O_h$  symmetry) that results in the overall  $T_d$  symmetry of  $Lu_2@C_{76}$ .

The above conclusion that the dynamical motion of metal atoms inside the carbon cage can make the EMF molecule to maintain the symmetry of the parent fullerene cage is rather general. Similar situations were widespread in the other EMFs, and herein we give some examples. In  $M_2@C_{80}$  ( $I_h$ ,  $M = La, Ce$ ) and  $Ce_2@C_{80}$  ( $D_{5h}$ ), the motion of metal atoms makes the whole molecule to maintain  $I_h$  or  $D_{5h}$  symmetry in the  $^{13}C$  NMR measurements.<sup>17,19-21,58,59</sup> In  $M@C_{82}$  ( $C_{2v}$ ,  $M = La, Y, Sc, Gd$ ), the motion of metal atoms makes the whole molecule to maintain  $C_{2v}$  symmetry.<sup>13-16,60-62</sup> In  $M@C_{74}$  ( $D_{3h}$ ,  $M = Ca, Y, La, Ba$  and  $Sr$ ), the energy minimum has a  $C_{2v}$  symmetry, while the  $^{13}C$  NMR showed  $D_{3h}$  cage symmetry due to the motion of metal atoms.<sup>63-68</sup> So far, all the experimental and theoretical

results obey this rule. Finally, we propose that the overall symmetries of EMFs are determined by the symmetry of carbon cage, and the motion trajectory of metal atoms will act in concert with the cage to keep the symmetry.

## Conclusions

By means of the relativistic DFT method and based on the representative patch of  $C_{76}(T_d)$ , we obtained the lowest-energy isomer of  $Lu_2@C_{76}$  (with a  $C_2$  symmetry). Our QTAIM analysis and the aromaticity evaluations showed that the formal electronic configuration of  $Lu_2^{4+}@C_{76}^{4-}$  rather than the traditional  $Lu_2^{6+}@C_{76}^{6-}$  can be inferred, which supports Yang *et al.*'s electronic structure assignment of  $Lu_2^{4+}@C_{76}^{4-}$ .<sup>23</sup> The good electron delocalization in  $C_{76}^{4-}(T_d)$  partially contributes to the thermodynamic preference of  $Lu_2@C_{76}(T_d)$ . We further located the transition state structure for the Lu motion between the lowest-energy isomers, and obtained the motion trajectory of Lu atoms inside the  $C_{76}$  cage. The rather small transition barrier leads to the flexible motion of the encapsulated Lu atoms inside the  $C_{76}$  cage, and the computed  $O_h$  symmetrical motion trajectory of the two Lu atoms is consistent with the STM image. We also discussed the formation of this motion trajectory by group theory in detail. Additionally, the <sup>13</sup>C NMR spectrum of  $Lu_2@C_{76}$  quantitatively computed by this trajectory also agrees well with the experimental data. Our detailed analysis of the experimental and theoretical results indicate that the overall symmetry of EMFs probably depends on the symmetry of carbon cage due to the dynamic motion of the encapsulated metal atoms.

## Acknowledgements

This work has been supported in China by the National Natural Science Foundation of China (Grant Nos. 21036006, 21137001, and 21373042) and the State Key Laboratory of fine chemicals (Panjin) project (Grant No. JH2014009), and in USA by National Science Foundation (Grant EPS-1010094) and Department of Defense (Grant W911NF-12-1-0083). The computational resources were provided by Shanghai Supercomputer Center.

## Notes and references

<sup>a</sup> State Key Laboratory of Fine Chemicals, Dalian University of Technology, Panjin, 124221, People's Republic of China

<sup>b</sup> Department of Chemistry, Institute for Functional Nanomaterials, University of Puerto Rico, San Juan, PR 00931, USA

\* Corresponding author. Email: haoce@dlut.edu.cn

- 1 T. Akasaka, and S. Nagase, *Endofullerenes: A New Family of Carbon Clusters[C]*. (Springer, 2002).
- 2 H. Shinohara, *Rep. Prog. Phys.* 2000, **63**, 843.
- 3 X. Lu, L. Echegoyen, A. L. Balch, S. Nagase, and T. Akasaka, *CRC Press*, 2014.
- 4 S. I. Kobayashi, S. Mori, S. Iida, H. Ando, T. Takenobu, Y. Taguchi, A. Fujiwara, A. Taninaka, H. Shinohara, and Y. Iwasa, *J. Am. Chem. Soc.* 2003, **125**, 8116.
- 5 T. Tsuchiya, R. Kumashiro, K. Tanigaki, Y. Matsunaga, M. O. Ishitsuka, T. Wakahara, Y. Maeda, Y. Takano, M. Aoyagi, T. Akasaka, M. T. H. Liu, T. Kato, K. Suenaga, J. S. Jeong, S. Iijima, F. Kimura, T. Kimura, and S. Nagase, *J. Am. Chem. Soc.* 2007, **130**, 450.
- 6 R. B. Ross, C. M. Cardona, D. M. Guldi, S. G. Sankaranarayanan, M. O. Reese, N. Kopidakis, J. Peet, B. Walker, G. C. Bazan, E. V. Keuren, B. C. Holloway, and M. Drees, *Nat. Mater.* 2009, **8**, 208.
- 7 A. A. Popov, S. Yang, and L. Dunsch, *Chem. Rev.* 2013, **113**, 5989.
- 8 X. Lu, T. Akasaka, and S. Nagase, *Acc. Chem. Res.* 2013, **46**, 1627.
- 9 P. Jin, C. Tang, and Z. Chen, *Coord. Chem. Rev.* 2014, **270-271**, 89.
- 10 L. Dunsch, and S. Yang, *Small* 2007, **3**, 1298.
- 11 L. Dunsch, and S. Yang, *The Electrochemical Society Interface*, 2006, **15**, 34.
- 12 J. Tang, G. Xing, Y. Zhao, L. Jing, H. Yuan, F. Zhao, X. Gao, H. Qian, R. Su, K. Ibrahim, W. Chu, L. Zhang, and K. Tanigaki, *J. Phys. Chem. B* 2007, **111**, 11929.
- 13 M. S. Golden, T. Pichler, and P. Rudolf, *Structure and Bonding*, 2004, **109**, 201.
- 14 W. Andreoni, and A. Curioni, *Phys. Rev. Lett.* 1996, **77**, 834.
- 15 E. Nishibori, M. Takata, M. Sakata, H. Tanaka, M. Hasegawa, H. Shinohara, *Chem. Phys. Lett.* 2000, **330**, 497.
- 16 P. Jin, C. Hao, S. Li, W. Mi, Z. Sun, J. Zhang, and Q. Hou, *J. Phys. Chem. A* 2007, **111**, 167.
- 17 T. Akasaka, S. Nagase, K. W. M. Kobayashi, K. Yamamoto, H. Funasaka, M. Kako, T. Hoshino, and T. Erata, *Angew. Chem. Int. Ed. Engl.* 1997, **36**, 1643.
- 18 E. Nishibori, M. Takata, M. Sakata, A. Taninaka, and H. Shinohara, *Angew. Chem. Int. Ed.* 2001, **40**, 2998.
- 19 J. Zhang, C. Hao, S. Li, W. Mi, and P. Jin, *J. Phys. Chem. C* 2007, **111**, 7862.
- 20 M. Yamada, T. Nakahodo, T. Wakahara, T. Tsuchiya, Y. Maeda, T. Akasaka, M. Kako, K. Yoza, E. Horn, N. Mizorogi, K. Kobayashi, and S. Nagase, *J. Am. Chem. Soc.* 2005, **127**, 14570.
- 21 M. Yamada, N. Mizorogi, T. Tsuchiya, T. Akasaka, and S. Nagase, *Chem. Eur. J.* 2009, **15**, 9486.
- 22 H. Umemoto, K. Ohashi, T. Inoue, N. Fukui, T. Sugai, and H. Shinohara, *Chem. Commun.* 2010, **46**, 5653.
- 23 T. Yang, X. Zhao, E. Osawa, *Chem. Eur. J.* 2011, **17**, 10230.
- 24 E. J. Baerends, J. Autschbach, A. Berces, C. B. P. M. Boerrigter, L. Cavallo, D. P. Chong, L. Deng, R. M. Dickson, D. E. V. Ellis, M. Faassen, L. Fan, T. H. Fischer, C. F. Guerra, A. J. S. van Gisbergen, J. A. Groeneveld, O. V. Gritsenko, M. Gru'ning, F. E. Harris, P. van den Hoek, H. Jacobsen, L. Jensen, G. van Kessel, F. Kootstra, E. van Lenthe, D. A. McCormack, A. Michalak, V. P. Osinga, S. Patchkovskii, P. H. T. Philipsen, D. Post, C. C. Pye, W. Ravenek, P. Ros, P. R. T. Schipper, G. Schreckenbach, J. G. Snijders, M. Sola, M. Swart, D. Swerhone, G. te Velde, P. Vernooijs, L. Versluis, O. Visser, F. Wang, E. V. Wezenbeek, G. Wiesenekker, S. K. Wolff, T. K. Woo, A. L. Yakovlev, and T. Ziegler, Amsterdam, The Netherlands, 2005.
- 25 G. te Velde, F. M. Bickelhaupt, E. J. Baerends, C. F. Guerra, S. J. A. V. Gisbergen, J. G. Snijders, and T. Zifgler, *J. Comput. Chem.* 2001, **22**, 931.
- 26 C. F. Guerra, J. G. Snijders, G. te Velde, and E. J. Baerends, *Theor. Chem. Acc.* 1998, **99**, 391.
- 27 B. Delley, *J. Chem. Phys.* 1990, **92**, 508.
- 28 E. V. Lenthe, R. V. Leeuwen, E. J. Baerends, and J. G. Snijders, *Int. J. Quantum Chem.* 1996, **57**, 281.
- 29 E. V. Lenthe, J. G. Snijders, and E. J. Baerends, *J. Chem. Phys.* 1996, **105**, 6505.
- 30 E. V. Lenthe, E. J. Baerends, and J. G. Snijders, *J. Chem. Phys.* 1994, **101**, 9783.
- 31 S. H. Vosko, L. Wilk, and M. Nusrir, *Can. J. Phys.* 1980, **58**, 1200.
- 32 A. D. Becke, *Phys. Rev. A* 1988, **38**, 3098.
- 33 J. Perdew, *Phys. Rev. B* 1986, **33**, 8822.
- 34 F. Biegler-König, AIM2000, version 1.0; University of Applied Sciences: Bielefeld, Germany, 2000.
- 35 R. F. W. Bader, *Atoms in Molecules: A Quantum Theory*, Oxford University Press, Oxford, U.K., 1990.
- 36 X. Cao, and M. Dolg, *J. Mol. Struct.: THEOCHEM* 2002, **581**, 139.
- 37 D. A. Pantazis, and F. Neese, *J. Chem. Theory Comput.* 2009, **5**, 2229.
- 38 J. P. Perdew, *Phys. Rev. B* 1986, **38**, 7406.
- 39 P. v. R. Schleyer, C. Maerker, A. Dransfeld, H. Jiao, and N. J. R. v. E. Hommes, *J. Am. Chem. Soc.* 1996, **118**, 6317.

- 40 Z. Chen, C. S. Wannere, C. Corminboeuf, R. Puchta, and P. v. R. Schleyer, *Chem. Rev.* 2005, **105**, 3842.
- 41 M. J. Frisch, G. W. Trucks, H. B. Schlegel, G. E. Scuseria, M. A. Robb, J. R. Cheeseman, G. Scalmani, V. Barone, B. Mennucci, G. A. Petersson, H. Nakatsuji, M. Caricato, X. Li, H. P. Hratchian, A. F. Izmaylov, J. Bloino, G. Zheng, J. L. Sonnenberg, M. Hada, M. Ehara, K. Toyota, R. Fukuda, J. Hasegawa, M. Ishida, T. Nakajima, Y. Honda, O. Kitao, H. Nakai, T. Vreven, J. A. Montgomery, Jr, J. E. Peralta, F. Ogliaro, M. Bearpark, J. J. Heyd, E. Brothers, K. N. Kudin, V. N. Staroverov, R. Kobayashi, J. Normand, K. Raghavachari, A. Rendell, J. C. Burant, S. S. Iyengar, J. Tomasi, M. Cossi, N. Rega, J. M. Millam, M. Klene, J. E. Knox, J. B. Cross, V. Bakken, C. Adamo, J. Jaramillo, R. Gomperts, R. E. Stratmann, O. Yazyev, A. J. Austin, R. Cammi, C. Pomelli, J. W. Ochterski, R. L. Martin, K. Morokuma, V. G. Zakrzewski, G. A. Voth, P. Salvador, J. J. Dannenberg, S. Dapprich, A. D. Daniels, Ö. Farkas, J. B. Foresman, J. V. Ortiz, J. Cioslowski, and D. J. Fox, Gaussian 09, revision A. 01. Wallingford, CT: Gaussian; 2009.
- 42 K. Wolinski, J. F. Hinton, and P. Pulay, *J. Am. Chem. Soc.* 1990, **112**, 8251.
- 43 A. G. Avent, D. Dubois, A. Pénicaud, and R. Taylor, *J. Chem. Soc., Perkin Trans.* 1997, **2**, 1907.
- 44 J. P. Perdew, K. Burke, M. Ernzerhof, *Phys. Rev. Lett.* 1996, **77**, 3865.
- 45 J. P. Perdew, J. A. Chevary, S. H. Vosko, K. A. Jackson, M. R. Pederson, D. J. Singh, C. Fiolhais, *Phys. Rev. B* 1992, **46**, 6671.
- 46 A. L. Svitova, K. B. Ghiassi, C. Schlesier, K. Junghans, Y. Zhang, M. M. Olmstead, A. L. Balch, L. Dunsch, and A. A. Popov, *Nat. Commun.* 2014, **5**, 3568.
- 47 P. R. Varadwaj, I. Cukrowski, and H. M. Marques, *J. Phys. Chem. A* 2008, **112**, 10657.
- 48 P. R. Varadwaj, and H. M. Marques, *Phys. Chem. Chem. Phys.* 2010, **12**, 2126.
- 49 B. Tan, R. Peng, H. Li, B. Wang, B. Jin, S. Chu, and X. Long, *J. Mol. Model.* 2011, **17**, 275.
- 50 A. A. Popov, and L. Dunsch, *Chem. Eur. J.* 2009, **15**, 9707.
- 51 P. R. Varadwaj, and H. M. Marques, *Theor. Chem. Acc.* 2010, **127**, 711.
- 52 P. R. Varadwaj, A. Varadwaj, G. H. Peshherbe, and H. M. Marques, *J. Phys. Chem. A* 2011, **115**, 13180.
- 53 Z. Badri, C. Foroutan-Nejad, and P. Rashidi-Ranjbar, *Comput. Theor. Chem.* 2013, **1009**, 103.
- 54 M. Bühl, and A. Hirsch, *Chem. Rev.* 2001, **101**, 1153.
- 55 Z. Chen, and R. B. King, *Chem. Rev.* 2005, **105**, 3613.
- 56 S. Osuna, M. Swart, and M. Solà, *Phys. Chem. Chem. Phys.* 2011, **13**, 3585.
- 57 A. A. Popov, and L. Dunsch, *Chem. Eur. J.* 2009, **15**, 9707.
- 58 K. S. Novoselov, A. K. Geim, S. V. Morozov, D. Jiang, Y. Zhang, S. V. Dubonos, I. V. Grigorieva, and A. A. Firsov, *Science* 2004, **306**, 666.
- 59 Z. Huang, X. Liu, K. Li, D. Li, Y. Luo, H. Li, W. Song, L. Chen, and Q. Meng, *Electrochem. Commun.* 2007, **9**, 596.
- 60 E. Nishibori, S. Narioka, M. Takata, M. Sakata, T. Inoue, and H. Shinohara, *Chemphyschem* 2006, **7**, 345.
- 61 L. Liu, B. Gao, W. Chu, D. Chen, T. Hu, C. Wang, L. Dunsch, A. Marcelli, Y. Luo, and Z. Wu, *Chem. Commun.* 2008, 474.
- 62 S. Guha, and K. Nakamoto, *Coord. Chem. Rev.* 2005, **249**, 1111.
- 63 J. Xu, T. Tsuchiya, C. Hao, Z. Shi, T. Wakahara, W. Mi, Z. Gu, and T. Akasaka, *Chem. Phys. Lett.* 2006, **419**, 44.
- 64 H. Oliver, H. Martin, G. Arthur, M. Michael, and D. P. J. Martin, *Z. Anorg. Allg. Chem.* 2005, **631**, 126.
- 65 S. Ren, D. Tian and C. Hao, *J. Mol. Model.* 2013, **19**, 1591.
- 66 T. Kodama, R. Fujii, Y. Miyake, S. Suzuki, H. Nishikawa, I. Ikemoto, K. Kikuchi and Y. Achiba, *Chem. Phys. Lett.* 2004, **399**, 94.
- 67 W. Zheng, S. Ren, D. Tian and C. Hao, *J. Mol. Model.* 2013, **19**, 4521.
- 68 S. Ren, D. Tian and C. Hao, *Comput. Theor. Chem.* 2013, **1020**, 57.